Int J Adv Manuf Technol (2008) 37:690–697
DOI 10.1007/s00170-007-1008-x

ORIGINAL PAPER

# The process simulation of virtual laser surface hardening

**Taohong Zhang · Tianyuan Xiao · Bingru Yang**

Received: 30 June 2006 / Accepted: 12 March 2007 / Published online: 27 April 2007


**Abstract** This paper focuses on solving the bottleneck problem-process simulation in virtual manufacture (VM), a solution of whole process simulation including geometrical aspect and physical aspect is put forward in the domain of laser surface hardening. For the difference of mechanisms among the different laser machining modes, the architecture integrated with the common and the distinction is constructed for the whole process simulation, and it is suitable for all laser machining modes. The virtual processing equipments for the laser machining are built by IGRIP software. The processing model is the map of the processing mechanism and the different models mapping to different machining modes. The whole process modeling of laser surface hardening is described. The extracted modeling parameters comprise geometrics, laser characters, material properties and mechanical properties, the model is built by artificial neural network method, and the finished model is embedded to IGRIP by quadric development. The whole virtual processing is implemented combining the whole model and the visualization simulation, the simulation result including the joints movement of the processing robot, collision-free report, processing effect prediction etc. are output. The analysis for the simulation result and the influence of parameters on processing effect are discussed to guide the real laser machining.

**Keywords** Artificial neural network · Laser surface hardening · The whole process modeling · The whole process simulation

This work is financially supported by the Key Projects for Device Development (No.[1997]167) and for Knowledge Innovation (No.KGCX1-11) of the Chinese Academy of Sciences, which are gratefully acknowledged.

T. Zhang (✉) · B. Yang
Information Engineering School,
University of Science and Technology Beijing,
Beijing 100083, People's Republic of China
e-mail: waterswordzth@163.com

T. Xiao
Department of Automation, Tsinghua University,
Beijing 100084, China

## 1 Introduction

With the conflict between people's need for various products and low cost, high quality, good service and the shorten of time-to-market for the new product more and more frequently, the importance of flexible manufacturing (FM) and virtual manufacture (VM) has gotten more and more attention [1, 2]. Due to the complexity, there is some difficultly to make VM into practice. One of the bottlenecks is the process simulation. As the kernel of VM, process simulation is at the bottom to reveal the essence of manufacturing [3]. The process simulation based on the techniques of modeling and simulation deals with the process, tooling and equipments etc. to analyze the factors which affect the process, product quality, processing time, costs and the relative motion between the equipment and the product. Due to the complexity of itself and many factors that must be considered, with the addition of the machining effect which is manifested by geometrical dimensions and machining accuracy, the early study of process simulation is emphasized on geometrical simulation. With the deepness of study, researches entered into the physical simulation. Machine tool agile manufacturing research is established funded by American NSF/ARPA combined many universities and companies [2] for the physical simulation. The machining modes include turning, milling, drilling etc., different modeling methods (analytical, experimental, mechanistic and numerical methods) are applied, and the force model, thermal model, wear model etc. are put forward [4–17]. However the real machining is a compositive process and can not be divided into isolated geometrical and physical aspects. The whole processing simulation should be accounted for to reveal the real machining mechanism. Anyway all these machining modes are limited to traditional mechanical modes. With the appearance of laser, laser processing has gained far-ranging application in industry and laser processing is an important constitute of manufacturing [18–22]. So the process simulation of laser processing should be included in VM. Now few researchers concentrated on this field.

The whole process simulation of laser surface hardening is presented in this paper. The architecture suitable for whole process simulation of laser surface hardening is introduced first. This architecture is also suitable for other laser processing operations. Then, the device model and the whole process model of laser surface hardening are built respectively. The parameters of the whole process model consist of the compositive geometrical, laser and material aspects and the modeling method is based on the artificial neural network. The process simulation is executed in the virtual environment made by IGRIP software and the simulation result is shown to provide the gist for the real laser hardening.

## 2 Architecture design

The process of laser surface hardening is sophisticated for it involves not only the movement of processing robot but the interaction of laser and material. The former is categorized into the geometrical simulation, and the simulation of the latter belongs to the physical simulation. The real laser surface hardening is a synthesized process and can not be divided into the geometrical or physical parts factitiously. For this complicated laser surface hardening process, an architecture which is suitable for the whole process simulation was constructed first. It is presented as Fig. 1. The architecture of the whole process simulation is comprised of three modules. One is the modeling module, the second is the simulation module, and the third is the simulation result and analysis module. The modeling module includes all the modeling involved in the laser surface hardening. It can be divided roughly into device modeling and process modeling. The device model refers not only to the laser machine but the accessorial device, namely the virtual manufacturing environment (as shown in Fig. 2). It can be divided into the geometrical model and the kinematical model according to the kinematics. The whole process modeling is built for the goal of the whole process simulation. Alos the modeling parameters conclude not only the geometrical parameters but also the physical parameters, concreted as laser parameters, material parameters and mechanical properties. After the models are established, it is going to the simulation module. The simulation results are reported and the analysis about the results is part of the third module.

The architecture in Fig. 1 has another advantage. It is suitable for other laser processing modes besides laser surface hardening. Although different laser processing modes mean the mechanisms of the interaction between laser and materials are different and different process models should be built for the different laser processing modes. However, laser processing is a kind of flexible machining, and different processing modes (cutting, wielding, rapid shaping, hardening etc.) can coexist in one laser processing system. So only the modeling parameters and the whole process model should be substituted in this architecture for other laser processing simulation. And the common device model and different process model can be embedded in one virtual environment.

## 3 Process simulation modeling

### 3.1 Device modeling

The device is comprised of movable components and unmovable components. The main devices in laser surface hardening system are laser machine, laser processing robot, workbench, the accessorial air equipment etc. The static devices (laser machine, workbench, accessorial air equipment) can be expressed by geometrical shape. For the movable device (laser processing robot), a kinematics is added for building the virtual device. The geometrical model is set up by CAD solid modeling function of IGRIP software or relative CAD software product. Kinematics of the device is added from the second development of SHARED LIBRARY in IGRIP. The device geometrical model is shown in Fig. 2. This laser processing robot is a frame robot with 5 axes (three translation axes $x,y,z$ and two rotating axes $A,C$). The kinematics of the robot is the conversion from the movement of five axes to the coordinates and direction cosine of robot end executor. The transformation formulas are listed below as Eq. 1–6.

$$x = P_x + \sin(\theta_A) l_w + a_x \cdot l_t \tag{1}$$

$$y = P_y - \cos(\theta_A) l_w + a_y \cdot l_t \tag{2}$$

$$z = P_z + a_z \cdot l_t \tag{3}$$

$$a_x = -\cos(\theta_A)\sin(\theta_C) \tag{4}$$

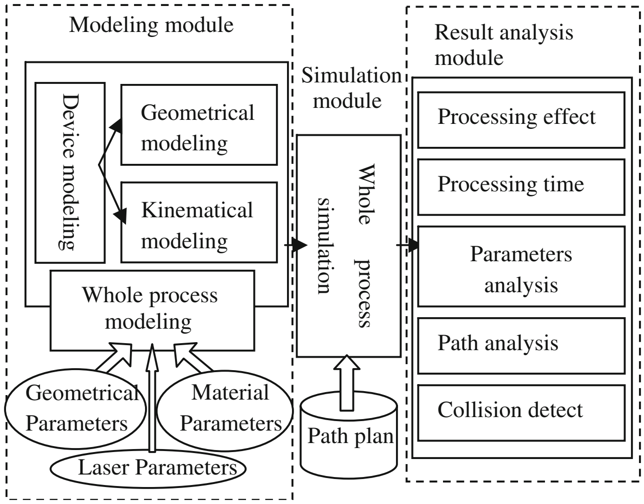


**Fig. 1** The architecture of whole processing simulation of laser machining

$$a_y = -\sin(\theta_A)\sin(\theta_C) \quad (5)$$

$$a_z = -\cos(\theta_c) \quad (6)$$

where $x$, $y$ and $z$ are the three coordinates of the processing point corresponding to the end executor, $a_x$, $a_y$ and $a_z$ are their direction cosine. $P_x$, $P_y$ and $P_x$ are the translation quantity of the three translation axes. $\theta_A$ and $\theta_C$ are the movement values of the two rotation axes. $l_w$ is the length of the tool-arm and $l_t$ is the length of the tool-head. The kinematics is programmed in C language and compiled into dynamic data library (DDL) for the calls of IGRIP SHARED LIBRARY.

## 3.2 Whole process modeling

The whole process modeling should consider the influence factors in the hardening processing thoroughly. The inputs of the model are the factors influencing the processing, and the outputs are the hardening effect. As shown in Fig. 3 the influent parameters of input can be abstracted into laser property, geometrical aspect and material aspect, and the mechanical properties and the use properties are the outputs. The goal of laser surface hardening is to promote the wear resistance, hardness and hardening depth to prolong the die life but not increase the surface roughness. So hardness, wear-resistance, hardening depth and surface roughness are extracted as the outputs of the model as shown in Fig. 3

(1) Laser parameters extraction

The laser beam for die surface hardening is transmitted after spatio-temporal translation to the die surface. The time character is the laser pulse shape and the pulse frequency. Square wave is adopted to harden the die surface and one square wave is used in one hardening spot, so the time parameters are laser power $P$ and the duration time $t$ of the square wave. The spacial translation is that the energy from a circle converted to a square dot-array distribution. A laser machine generates a circular laser beam with a spatial distribution of the Gaussian type, leading to a processed area of a circular spot on the object. If this laser beam is used for hardening without any modification, the center area of the circular spot will melt due to overheating while the boundary of the spot is not hardened enough. Therefore the processing laser beam for die-surface hardening is often transformed uniformly into a square distribution. Figure 4 shows that the laser energy distributed in a circle is transformed into a distribution with many small circles, which are arranged into a square pattern; known as the dot-

**Fig. 2** Model of laser machining device

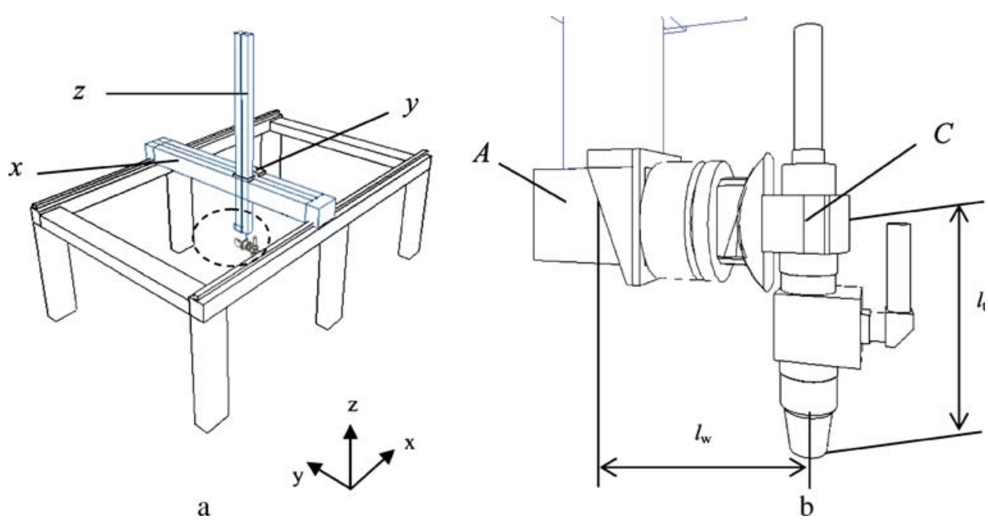

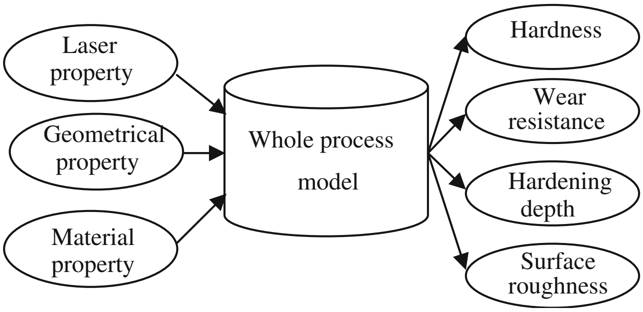


**Fig. 3** The whole process model frame of laser surface hardening

array distribution. The laser energy contained in each small circle also has a Gaussian distribution and the total energy is unvaried. Another advantage of the dot-array distribution is that perfect adjacence of the laser square spot can be achieved. With a square laser spot, the workpiece surface can be hardened uniformly [23]. The dot array in Fig. 4 is 7×7, it can be generalized to $b\times b$. The appearance of the processed area is a square spot with sides of $a\times a$. Therefore one parameter called dot-array dimension $h$ can be named to express the spacial feature

$$h=\frac{a\times a}{b\times b}. \tag{7}$$

(2) Geometrical parameters extraction

The processing mode of laser surface hardening is that the laser beam with spatio-temporal translation is projected to the die surface. The side of the projected surface is as low as millimeter, and the variation of curvature is not much due to the smoothness requirement of the surface, so the projected surface can be replaced by a projected plane. Based on this replacement, the processed area can be treated as a point. The ideal processing is that the laser beam projects to this point with ideal distance and ideal angle (along the normal of this point). However, in real processing, most surfaces of the die are free surface, so the laser tool-head can not access the ideal point due to the collisions which happened. Therefore the processing laser beam deviates from the ideal position some distance and/or angle. The sketch is shown in Fig. 5 in which A represents the processing point, $P_{\mathrm{i}}$ the ideal processing point, and $P_{\mathrm{r}}$ the real processing point. It can be obtained from two parameters of deviation angle θ (which is the included

**Fig. 4** Special laser beam dot-array distribution and the appearance of the processed area

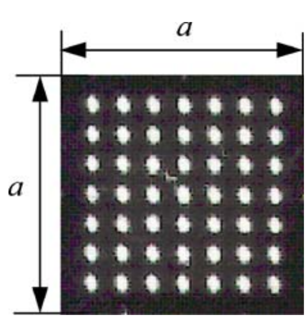


**Fig. 5** The ideal processing position and real processing position

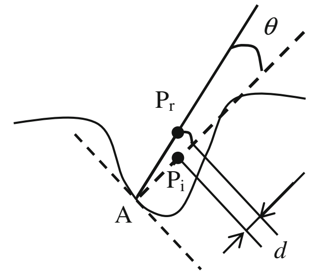


angle of line $AP_{\mathrm{r}}$ and line APi) and offset distance d. d is the difference between distances of $AP_{\mathrm{r}}$ and $AP_{\mathrm{i}}$.

$$d=\overline{AP}_r-\overline{AP}_i \tag{8}$$

(3) Material property extraction

Material property can be expressed by different manners such as chemical constitutions, microstructures etc. However the phase of the microstructure can inflect the essence of material. This paper extracts the volume proportion of microstructure to stand for the material property. By analysis, the microstructures of autobody die are pearlite, cementite, ferrite, graphite, and iron phosphide eutectic [24, 25].

(4) Neural network approach for modeling

For the complicated non-linear process, the neural network approach is a preferred choice. Within the last decade the number of applications of neural networks within the manufacturing field has steadily increased. A number of recent reviews have identified a diverse range of manufacturing applications [26–29]. This paper adopts the back propagation (BP) network [30] to build the whole process model. The BP neural network is comprised of a number of inputs, hidden layer neurons, and outputs. Each neuron has a transfer function and bias that relates its input to its output. Sigmoid transfer functions are employed in this paper. The input parameters as above extracted are laser power ($P$), laser during time ($t$), dot-array dimension ($h$), deviation angle (θ), offset distance ($d$), and volume proportion of microstructure pearlite, cementite, ferrite,

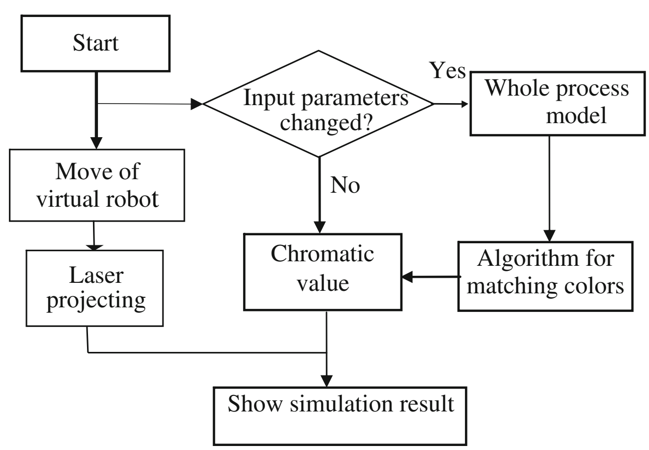


**Fig. 6** Flow chart of whole process simulation

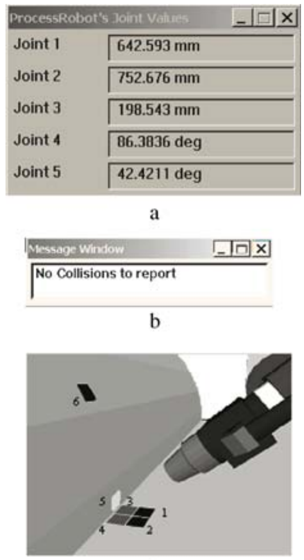


**Fig. 7** The visualization display of the simulation result. (**a**) The movement of virtual laser process robot in the simulation. (**b**) The collision detection report. (**c**) The visualization display of the processing effect (hardness)

graphite, iron phosphide eutectic. The inputs are amounts upto 10. The outputs are hardness, relative wear resistance, hardening depth and surface roughness, i.e., the output amount is 4. The sample data was randomly split into a training set and a test set. The number of hidden layers is set to 2, and every layer has 5 cells. Training was performed using a relatively large number of epochs (10 000) and a long time would be needed (the exact period depends upon the speed of the processor employed). However, it is important to note that this time requirement applies only to the training operation, and that once the network is trained it can provide simulation result quickly and easily. After pass the examination of test set, the model can be accepted satisfactorily.

## 4 Simulation

After the virtual device and the whole process model are established, the whole process simulation can be implemented in the virtual environment. The processing trail was set to the virtual robot. At every processing point, the processing parameters are inputted to the whole process model. If the input parameters are the same as that of the former point, the whole process model is not called in the simulation and the simulation result remains unchanged, or the whole process model is called to calculate the simulation result. The chromatic value is matched by RGB of computer. The simulation flow can be shown in Fig. 6. The movement of the virtual laser robot is reported as shown in Fig. 7(a). If collision happens in the process, alarming color is displayed, or no-collision detection report is shown in Fig. 7(b). The predicted processing effect (hardness) of simulation result is visualized in the simulation environment. In Fig. 7(c) the point 1, point 2 and the point 6 (coated by red color) stand for the hardness over HV800, the hardness of point 3 and point 4 (coated by orange color) is between HV800~600, and the hardness of point 5 (coated by green color) is in the range of HV600~400.

## 5 Simulation result analysis

### 5.1 Discussion of the predicted result

The movement of the laser process robot can be tested in the virtual process and guide for the off-line programming of robot. Collision detect avoids great machining accident. When collision happened in the simulation, the trail must be adjusted, and the new trail is inputted again to the virtual device for simulation, this process repeats until the report of collision free (Fig. 7b) appears. The simulation time from the virtual process can provide a reference for promoting the real process efficiency. The processing effects such as hardness, hardening depth etc., are predicted.

The simulation result after the whole process simulation is more precise than that from only physical simulation. It can be demonstrated from the comparison of simulation result with geometrical parameters or without. One case is with the input geometrical parameter $d$=1.9 mm, $\theta$=8°, the other is without geometrical parameter, it can be seen as $d$=0 mm, $\theta$=0°. The other parameters are laser power $P$=2000 W, laser duration time $t$=70 ms, dot-array dimension $h$=0.6 mm, volume proportion of microstructure pearlite

**Table 1** Comparison of simulation result

| | | | Processing effect predict | | |
|---|---|---|---|---|---|
| | | Hardness (HV) | Hardening depth (μm) | Relative wear resistance | Surface roughness (Ra) |
| Experiment value | | 621 | 340 | 2.1 | 1.7 |
| Simulation 1 | $d$=1.9 mm $\theta$=8° | 688 | 410 | 2.5 | 1.7 |
| | Relative error | 11% | 21% | 19% | 0% |
| Simulation 2 | $d$=0 mm $\theta$=0° | 920 | 502 | 3.48 | 1.7 |
| | Relative error | 48% | 48% | 66% | 0% |

75%, cementite 1%, ferrite 20%, graphite 3%, iron phosphide eutectic 1%. The compare of simulation result is shown in Table 1. From this table , it can be seen that the average relative error is reduced from 54% to 17%.

### 5.2 Parameters influence analysis

To avoid the processing fault, the amending method is adjusting the process parameters, but how the parameters influence the processing effects should be clarified first. To demonstrate the influence of one certain parameter distinctly, it is designed that all parameters remain unchanged except that parameter. From the contrast of simulation result, the influence on the processing effect of that parameter can be obtained. Here three parameters are analyzed.

(1) The influence of laser duration time

In the input parameters, the laser duration time varies while others keep fixed, i.e., $P$=2000 W, $d$=0 mm, θ=0°, $h$= 0.6 mm, volume proportion of microstructure is the same as the values listed above. The laser duration time increases from 10 ms to 90 ms, the hardness, hardening depth, and surface roughness are all changed. The change trend is shown in Fig. 8. With the increase of laser duration time, the hardness increases, and the hardening depth increases too at the beginning. But at $t$=80 ms, the surface roughness decreases, which accounted for melt happened on the surface, so the hardening depth decreased when $t$ is greater than 80 ms.

(2) The influence of offset distance

The parameter of offset distance varied from 0 to 3.0 mm while other parameters unvaried as above. The processing effect under these parameters is graphed in Fig. 9. From this figure, we can see that the processing effect changed little when the value of offset distance was small. It meant the processing effect was not influenced when the laser toolhead left off the ideal position in a little range. When the offset distance increased gradually to 2 mm, the hardness and the hardening depth dropped greatly. It meant the energy of the laser beam dissipated so greatly that it lost the ability of machining. It can be obtained that the distance of 2 mm was the critical value.

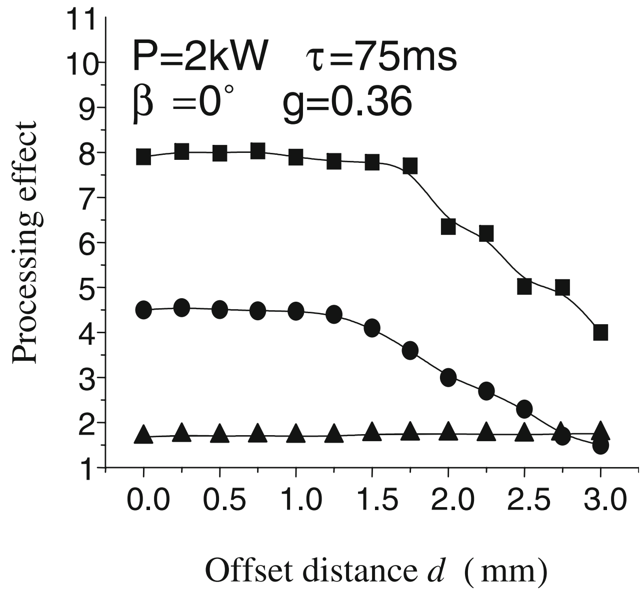


**Fig. 9** The influence on processing effect of deviation distance. ■ hardness (×100 HV), ● hardening depth(×100 μm), ▲ surface roughness (Ra)

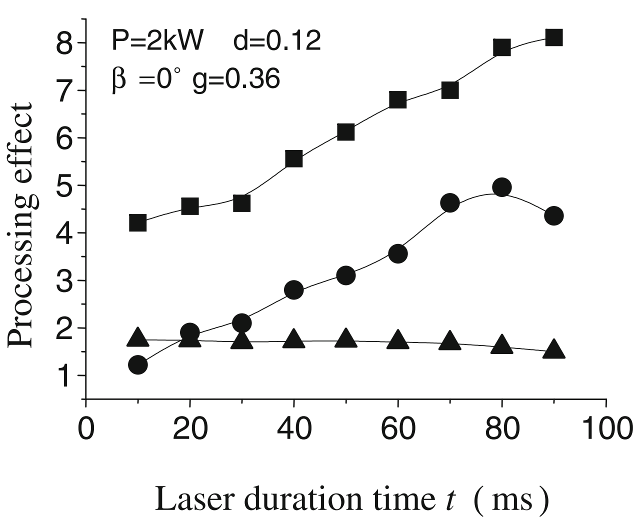


**Fig. 8** The influence on processing effectof laser duration time. ■ hardness (×100 HV), ● hardening depth (×100 μm), ▲ surface roughness (Ra)

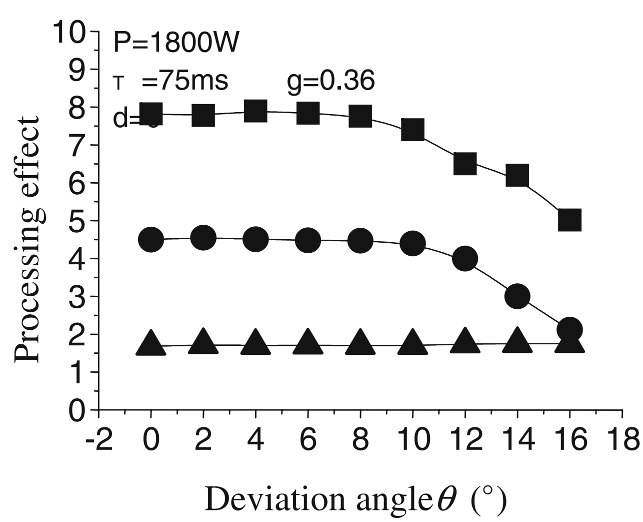


**Fig. 10** The influence on processing effect of deviation angle. ■ hardness (×100 HV), ● hardening depth (×100 μm), ▲ surface roughness (Ra)

(3) The influence of deviation angle

The ideal processing angle of the laser surface hardening is the laser beam projected to the normal of the processed point, at that time the energy of the laser beam is absorbed maximumly. When the processing angle is deviated from the ideal direction, the processing effect will be affected. The detailed degree of the affection is figured in Fig. 10. From the figure it can be seen that the processing effort varied little with a few increases of deviation angle. It meant the laser energy remained unconsumed. With the continuous increase of the deviation angle, it can be found that the affection for hardness, hardening depth, and the surface roughness is not serious within the scope of 10°. However, when the deviation angle is larger than 10°, the surface roughness stayed unvaried, however the hardness, hardening depth dropped rapidly. That meant all the laser energy dissipated and it led to the obvious shortage of processing. So the processing parameters must be adjusted for the satisfied machining.

## 6 Conclusions and perspectives

In this paper, the whole process simulation on the laser surface hardening domain is probed. For the flexibility of laser processing, a flexible architecture for this kind of flexible machining is presented. For different laser processing mode, the different whole process model is embedded into the whole structure. The whole process modeling is not the solely geometrical or physical aspect at all, main factors including geometry, laser parameters, material parameters and mechanical properties are considered together to map the real laser hardening. Artificial neural network approach is used to build the whole process model which is embedded into the simulation system developed by IGRIP software. The study has demonstrated that the neural networks are suitable to this non-liner laser processing. The whole process simulation is implemented in the virtual environment and the output of simulation result including the movement of processing robot, running time, collision-free report, process effect predict, etc. From the comparison of simulation results, the value demonstrates that the whole process simulation is more effective than only physical simulation. The analysis of parameters provides a significant reference for the real machining and for the optimization of the processing.

The future research is to perfect the whole process simulation system including other whole process models mapping to the corresponding laser processing modes (such as welding, cutting etc.), the addition of the feedback happened in the processing, the method for avoiding collision intelligently embedded into the system etc. The method for the whole process modeling can be diversiform to integrate into the simulation system.

**Acknowledgements** The authors would like to thank Shanghai Volkswagen Company for providing the autobody dies. The authors are also grateful to Chinese Academy of Sciences for fund support.

## References

1. Nagel R and Dove R (1991) 21st century manufacturing enterprise strategy, an industry-led view. Technical report, Iacocca Institute, Lehigh University, USA
2. NSF/ARPA, Machine tool agile manufacturing research, http://mtamri.me.uiuc.edu/technicalprogrames/processmodeljuly95.html
3. Kimura P (1993) Product and process modeling as a Kernel for virtual manufacturing environment. Ann CIRP 42:85–93
4. Ehmann KF, Kapoor SG, DeVor RE, Lazoglu I (1997) Machining process modeling: a review. J Manuf Sci Eng 119:655–663
5. Parakkal G, Zhu R, Kapoor SG, DeVor RE (2002) Modeling of turning process cutting forces for grooved tools. Int J Mach Tools Manuf 42:179–191
6. Mehdi K, Rigal JF (2004) A numerical model for cutting process simulation and prediction of cutting forces in peripheral milling. IEEE International Conference on Industrial Technology (IEEE Cat. No. 04TH8771) 2:734–40
7. Yang Y, Feng K, Bi L, Jiang YM, Feng B (2004) The 3D numerical simulation of stress field coupled with temperature field in cutting process. 2004 International Conference on Intelligent Mechatronics and Automation (IEEE Cat. No.04EX952), pp 739–741
8. Sushanta KS, Ozdoganlar OB, Richard ED and Kapoor SG (2003) Effect of groove-type chip breakers on twist drill performance. Int J Mach Tools Manuf 43:617–627
9. Bason EC, Yung CS (2002) A comprehensive chatter prediction model for face turning operation including tool wear effect. Int J Mach Tools Manuf 42:1035–1044
10. Balkrishna CR, Yung CS (1999) A comprehensive dynamic cutting force model for chatter prediction in turning. Int J Mach Tools Manuf 39:1631–1654
11. Ko JH, Yun WS, Cho DW, Ehmann KF (2002) Development of a virtual machining system, part 1: approximation of the size effect for cutting force prediction. Int J Mach Tools Manuf 42:1595–1605
12. Yun WS, Ko JH, Cho DW, Ehmann KF (2002) Development of a virtual machining system, part 2: prediction and analysis of a machined surface error. Int J Mach Tools Manuf 42:1607–1615
13. Yun WS, Ko JH, Lee HU, Cho DW, Ehmann KF (2002) Development of a virtual machining system, part 3: cutting process simulation in transient cuts. Int J Mach Tools Manuf 42:1617–1626
14. Smith S, Tlusty J (1990) Update on high-speed milling dynamics. ASME J Eng Ind 112:142
15. Jiaa CL, Dornfeld DA (1998) A self-organizing approach to the prediction and detection of tool wear. ISA Trans 37:239–255
16. Cao T, Sutherland JW (2002) Investigation of thread tapping load characteristics through mechanistics modeling and experimentation. Int J Mach Tools Manuf 42:1527–1538
17. Zhao H, Ehnamm KF (2003) Mechanistic model for spade drills for wood drills operations, part1: model development. J Manuf Sci Eng 125:226
18. Kolbe CM (1990) Widefield-application of lasers for the surface treatment of metallic components. Mach Market 96:52–57

19. Grob MS, Black I, Muller WH (2001) 26th European conference on laser interaction with matter. Proc SPIE 44:236–239
20. Komanduri R, Hou ZB (2001) Thermal analysis of laser surface transformation hardening. Int J Heat Mass Transfer 44:2845–2862
21. Woodard PR, Dryden J (1999) Thermal analysis of a laser pulse for discrete spot surface transformation hardening. J Appl Phys 85:2488–2496
22. Ion JC (2002) Laser transformation hardening. Surf Eng 18:14–31
23. An YQ, Yu G (1999) Laser surface treatment of carbon steels using diffractive optical converters. Proc. SPIE, AHPLA'99, Japan
24. Roy A, Manna I (2001) Laser surface engineering to improve wear resistance of austempered ductile iron. Mater Sci Eng A 297 (1–2):85–93
25. Levcovici SM, Levcovici DT, Munteanu V (2000) Laser surface hardening of austenitic stainless steel. J Mater Eng Perform 9 (5):536–540
26. Udo GJ (1992) Neural network applications in manufacturing processed. Compu Ind Eng 23:97–100
27. Zhang H, Huang SH (1995) Applications of neural networks in manufacturing: a state-of-the-art survey. Int J Prod Res 33:705–728
28. Guessasma S, Montavon G, Coddet C (2004) Modeling of the APS plasma spray process using artificial neural networks: basis, requirements and an example. Comput Mater Sci 29:315–333
29. Smith LN, German RM, Smith ML (2002) A neural network approach for solution of the inverse problem for selection of powder metallurgy materials. J Mater Process Technol 120:419–425
30. Jain C, Vemuri VR (Eds.), Industrial Applications of Neural Networks, Boca Raton: CRC Press LLC, 1999, ISBN 0-8493-9802-9